Available online at BCREC website: https://bcrec.id

Bulletin of Chemical Reaction Engineering & Catalysis, 15 (2) 2020, 568-578

Research Article

Dehydrogenation of Cyclohexanol to Cyclohexanone Over Nitrogen-doped Graphene supported Cu catalyst

Alyaa K. Mageed[1,*], Dayang A.B. Radiah[2], A. Salmiaton[2], Shamsul Izhar[2], Musab Abdul Razak[2], Bamidele Victor Ayodele[3,*]

[1]Department of Chemical Engineering, University of Technology, Baghdad, Iraq.
[2]Department of Chemical and Environmental Engineering, Faculty of Engineering, Universiti Putra Malaysia, 43400, Serdang, Selangor, Malaysia.
[3]Institute of Energy Policy and Research, Universiti Tenaga Nasional, Jalan IKRAM-UNITEN 43000, Kajang, Selangor, Malaysia.

Received: 16th December 2019; Revised: 9th July 2020; Accepted: 9th July 2020; Available online: 30th July 2020; Published regularly: August 2020

Abstract

In this study, the dehydrogenation of cyclohexanol to cyclohexanone over nitrogen-doped reduced graphene oxide (N-rGO) Cu catalyst has been reported. The N-rGO support was synthesized by chemical reduction of graphite oxide (GO). The synthesized N-rGO was used as a support to prepare the Cu/N-rGO catalyst via an incipient wet impregnation method. The as-prepared support and the Cu/N-rGO catalyst were characterized by FESEM, EDX, XRD, TEM, TGA, and Raman spectroscopy. The various characterization analysis revealed the suitability of the Cu/N-rGO as a heterogeneous catalyst that can be employed for the dehydrogenation of cyclohexanol to cyclohexanone. The catalytic activity of the Cu/N-rGO catalyst was tested in non-oxidative dehydrogenation of cyclohexanol to cyclohexanone using a stainless-steel fixed bed reactor. The effects of temperature, reactant flow rate, and time-on-stream on the activity of the Cu/N-rGO catalyst were examined. The Cu/N-rGO nanosheets show excellent catalytic activity and selectivity to cyclohexanone. The formation of stable Cu nanoparticles on N-rGO support interaction and segregation of Cu were crucial factors for the catalytic activity. The highest cyclohexanol conversion and selectivity of 93.3% and 82.7%, respectively, were obtained at a reaction temperature of 270 °C and cyclohexanol feed rate of 0.1 ml/min.

Keywords: Cyclohexanol; Cyclohexanone; Copper; dehydrogenation; Nitrogen-doped reduced graphene oxide

How to Cite: Mageed, A.K., Radiah, D.A.B., Salmiaton, A., Izhar, S., Razak, M.A., Ayodele, B.V. (2020). Dehydrogenation of Cyclohexanol to Cyclohexanone Over Nitrogen-doped Graphene supported Cu catalyst. *Bulletin of Chemical Reaction Engineering & Catalysis*, 15(2), 568-578 (doi:10.9767/bcrec.15.2.6774.568-578)

Permalink/DOI: https://doi.org/10.9767/bcrec.15.2.6774.568-578

1. Introduction

The dehydrogenation of cyclohexanol to cyclohexanone is an important reaction for the production of chemical intermediates used for the synthesis of caprolactam, nylon and, polyamide [1]. The industrial-scale cyclohexanone production has been made possible using Cu-Mg and Cu-Zn-Al catalysts [2]. The dehydrogenation of cyclohexanol over these catalysts were reported to give conversions ranged 50-60% and

* Corresponding Author.
E-mail: 80077@uotechnology.edu.iq (A.K. Mageed); ayodelebv@gmail.com (B.V. Ayodele)

cyclohexanone selectivity of 99% [3]. However, cyclohexanol dehydrogenation has been limited by the reversibility phenomenon of the dehydrogenation reaction which has been reported to keep the cyclohexanol conversion to 50-60% at 250 °C [3]. To overcome this limitation, Cu-based catalysts have been investigated for dehydrogenation of cyclohexanol to cyclohexanone [4,5]. Attempt in improving the cyclohexanol conversion using these catalysts resulted in a decrease in the selectivity of cyclohexanone due to an increase in the formation of impurities such as phenol and cyclohexene as by-products [6].

The use of support for the synthesis of Cu catalyst has been shown to improve cyclohexanol conversion and cyclohexanone selectivity [7]. This was due to the efficient dispersion of the Cu on the support. Simon *et al.* [4] reported that ZnO and MgO supported Cu catalysts with high loading were found to have high conversion and selectivity, thereby overcoming the limitations in the cyclohexanone production process [4]. Graphene, a two-dimensional carbon nanostructure has many excellent properties such as outstanding charge carrier mobility, thermal and chemical stability, high specific surface area, and superior stability [8,9] could be appropriate support material for the dispersion of Cu. Hence, the dispersion of Cu on the surface of reduced graphene oxide could form the basis for the development of new catalytic material for dehydrogenation of cyclohexanol. To the best of the author's knowledge, there is no reported work on the dehydrogenation of cyclohexanol over nitrogen-modified RGO supported Cu catalysts. The modification of the RGO with nitrogen to give N-rGO is expected to enhance the Cu-based catalytic activity and stability [10,11].

The present study, therefore, focuses on the synthesis of N-rGO nanosheets supported Cu catalyst which was prepared as a form of paper, whereas most of the catalytic studies are available as powder forms. The paper-like form of catalysts presents an opportunity ease of handling during an industrial application compared to the powdery form. Besides, the exceptional porous nature of the paper-like catalyst could significantly influence the catalytic activities. Therefore, in this work, the catalyst was prepared in a new paper form and the catalyst performance was evaluated in terms of activities and stability of the synthesized catalyst during catalytic gas-phase dehydrogenation reaction of cyclohexanol to cyclohexanone at the moderate temperatures.

2. Materials and Methods

2.1 Chemicals

The chemical used in this study were purchased from different manufacturers at various purity grades: Purified graphite powder, concentrated H_2SO_4, (MW = 98.07 g.mole^{-1}, 98%, Sigma-Aldrich), concentrated HNO_3, (MW = 63.01 g.mole^{-1}, 65%, Fisher Scientific) and $KClO_3$, (MW = 122.5495 g.mole^{-1}, 99%, Fisher Scientific), NH_3 solution (MW = 17.03 g.mole^{-1}, 30%, Analytical grade - Sigma-Aldrich), were used for the synthesis of the reduced graphene oxide. Copper nitrate trihydrate ($Cu(NO_3)_2.3H_2O$); MW = 241.60 g.mole^{-1}, Sigma-Aldrich) was used as the Cu precursor. Cyclohexanol (MW = 100.16 g.mole^{-1}, 99.5%, Sigma-Aldrich) was used as the reactant chemical and standard. Cyclohexanone (MW = 98.15 g.mole^{-1}, 99.5%, Sigma-Aldrich) was also used as standard.

2.2 Preparation of Catalysts

Before the preparation of the catalyst, the N-rGO support was synthesized by chemical reduction of GO in NH_3 environment followed by thermal treatment with N_2. The Cu/N-rGO was prepared by incipient wet impregnation. The support (GO) was prepared from natural graphite flakes using modified Staudenmaier's method as reported by Lee and Seo [12]. For the preparation of the GO, an ice-cooled 2:1 mixture of H_2SO_4 and HNO_3 was mixed with a stipulated amount of natural flake graphite. The mixture was allowed to react with temperature-controlled at 30 °C with the addition of $KCLO_3$. Stipulated amount of deionized water was added to the mixture after 96 h and the mixture was filtered using a nylon membrane to obtain a precipitated GO. The GO was subsequently washed with HCl solution for removal of sulfite ions impurities and thereafter washed with deionized water to remove any form of chloride ions. The resulting graphite oxide was then exfoliated and reduced to graphene oxide by mixing with NH_3 solution for 1 h and thereafter refluxed at 130 °C for 3 h. The resulting rGO was subsequently calcined at 200 °C in the N_2 environment for 40 minutes to obtain nitrogen-doped reduced graphene oxide (N-rGO). The thermal method was based on that described by Ning *et al.* [13].

The Cu/N-rGO catalyst was synthesized using incipient wetness impregnation of the Cu-precursor into the N-rGO support. The mass of the impregnated precursor was calculated to obtain an equivalent amount of 1 wt% of Cu.

The wet slurry containing the Cu-precursor and the N-rGO support was dried overnight at 110 °C, calcined, and subsequently reduced in the N_2/H_2 (10% (v/v)) environment at 275 °C for 3 h to obtain as-synthesized 1 wt% Cu/N-RGO catalyst.

2.3 Characterization of Catalysts

Field emission scanning electron microscopy (FESEM, JSM-7600 F) and transmission electron microscopy (TEM, Hitachi, H-7100) were used for the morphological analyses of the supports (GO, N-rGO) and the Cu/N-rGO catalyst. Prior to the TEM analysis, the catalyst sample was sonicated in absolute ethanol, dried at room temperature (25 °C), and then placed on a carbon-coated copper grid. The elemental composition of the sample was analyzed by energy-dispersive X-ray spectroscopy (EDX) (JSM-7600 F). A programmed thermal stability test of the catalyst sample was examined under a nitrogen atmosphere using thermogravimetric analysis (TGA) (TA instrument, Q50). To quantify the defects in the product materials, Raman spectra were measured using an excitation wavelength of 532.027 nm provided by a Spectra Model Alpha 300R and brand WI Tec. The X-ray diffraction (XRD) of the catalysts was measured to determine its crystallinity. Using a 2θ scanning range of 3° to 180°, the diffractogram was recorded by RIGAKU miniflex II equipped with the latest version of PDXL, RIGAKU full function powder-diffraction analysis software having Cu Kα X-ray source and wavelength (λ) of 0.154 nm.

2.4 Catalytic Activity

The reaction study showing the catalytic activity of the Cu/N-rGO catalyst in the dehydrogenation of cyclohexanol to cyclohexanone was performed in a continuous flow fixed bed reactor. The reaction was performed at atmospheric pressure (1 atm). The schematic representation of the experimental setup is depicted in Figure 1. The fixed bed reactor was connected to a nitrogen gas cylinder which serves as the carrier gas and to a liquid micropump for the feeding of the cyclohexanol into the reactor. Approximately 100 mg of the prepared catalyst was loaded into the fixed bed reactor. The reactor which is a stainless steel tube was vertically placed in a furnace heated by an external electric heater and insulated with glass wool. The temperature of the catalytic bed was monitored using a K-type thermocouple. The dehydrogenation process was performed at a temperature range of 200-270 °C, weight hour space velocity (WHSV) of 57 and 114 $h^{-1,}$ and gas hourly space velocity (GHSV) of 1580 h^{-1}. The WHSV was calculated as the weight of feed flow per unit weight of the catalyst per hour while the GHSV was calculated as the hourly volumetric feed gas flow rate/reaction volume. The vapor effluent from the reactor was cooled down to 25 °C to enhance the separation of the gas and liquid products. The liquid and gas products were collected at node 10 (Figure 1). The liquid products were analyzed using GC/FID (CP-Sil 24 CB 30 m × 0.25 mm × 0.25 um).

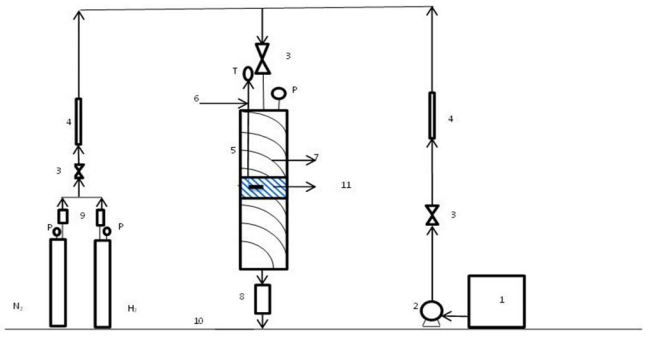

Figure 1. Diagram showing the experimental setup.

3. Results and Discussion

3.1 Morphology Analysis

The representative FESEM and TEM analysis showing the morphology of the Cu/N-rGO catalyst are depicted in Figures 2 and 3 respectively. Interestingly, the GO obtained from the acid oxidation was formed by a few layers of GO as shown in Figure 2. A similar observation was also reported by Loryuenyong *et al.* [14]. It can be seen from the FESEM micrographs that the formed N-rGO nanosheets have distinctive corrugated features. However, this corrugated feature was subsequently transformed into a wavy shape with extended sheets of lateral dimensions ranging from a few micrometers to tens of micrometers in length with layered structures. The effects of doping the GO with Nitrogen were quite apparent in which well-exfoliated samples were formed as shown in Figure 2(b) [15]. Functioning the exfoliated sheets with the copper salt and further calcined in the N_2/H_2 atmosphere had exfoliated the sheet further. The morphology of the Cu/N–rGO nanosheets formed is depicted in

Figure 2(c). With the dispersion of the 1 wt%Cu, the compacted shaped of the N-rGO was leavened and formed a lightweight foam-like structure, the findings as in [16].

The TEM image of the GO (Figure 3(a)) shows that each visible GO flake is comprised of few layers of GO sheet stacked laterally. The image of the GO formed revealed thin and wrinkle nanosheets such that it could allow the passage of electron beam [14]. The GO nanosheets also had crumple and ripple structures and in the lateral size ranged from nanometers up to a few micrometers as that described by [17]. The appearance of these features might be due to the deformation of the graphite oxide layers that occurred during the exfoliation and restacking processes.

The modification of the reduced GO with Nitrogen displayed a corrugated effect on the GO resulting in isolated small fragments on the surface as shown by the TEM image in Figure 3(b) [18,19]. This observation is consistent with the formation of multilayer structure as shown by the TEM image in Figure 3(c) [20] which could be attributed to the defect structure formed upon exfoliation and the presence of foreign nitrogen atoms [21]. Furthermore, a well-dispersed Cu nanoparticle is noticeable on the surface of N-rGO as presented by TEM images in Figure 3 (d and e) [16]. The particle size distribution revealed that the Cu nanoparticles were in the range of 5.0 nm to 50.0 nm with a mean diameter of 27.5 nm [22].

3.2 Energy-Dispersive X-ray Spectroscopy Analysis (EDX)

The elemental compositions of GO, N-rGO, and Cu/N-rGO catalysts obtained from the EDX analysis are shown in Table 1 and the micrographs of the samples are shown in Figure 4. Interestingly, all components (C, O, N, and Cu) were found in the proportions of 76.06 wt%, 14.86 wt%, 7.22 wt%, and 1.86 wt%, respectively. The results also confirmed that the oxygen-containing functional groups could be removed during the N-doping process with the ratio (Cu/C) of 0.024) [23−25].

3.3 Thermal Gravimetric Analysis

The TGA profile showing the thermal behavior of the as-prepared GO, N-rGO, and Cu/N-rGO sheets under the temperature-programmed calcination environment is depicted in Figure 5. The temperature-programmed calcination was conducted in a flow of nitrogen at a temperature range of 50−900 °C. The GO exhibits more than 80% weight loss between 100-470 °C resulting from the removal of the labile oxygen-containing functional groups, such as CO, CO_2, and H_2O vapors. The N-rGO sheets show much higher thermal stability with mass loss up to 262 °C. The mass loss ob-

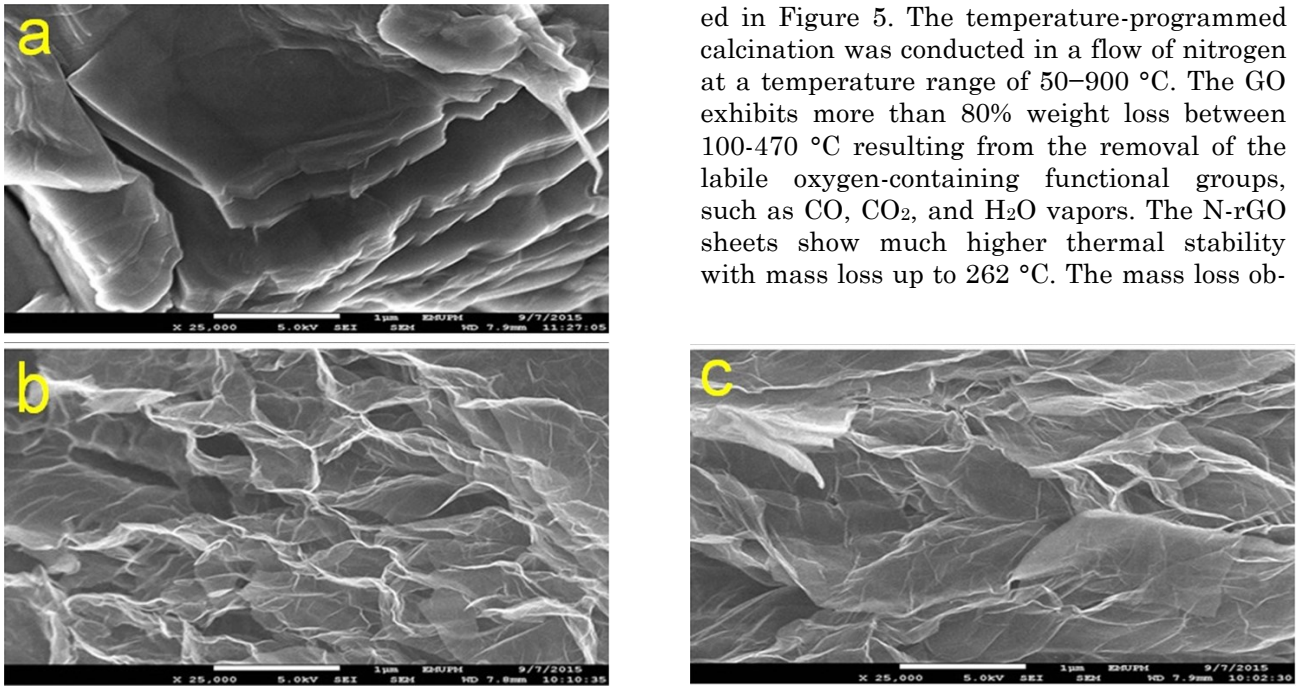

Figure 2. FESEM of (a) GO, (b) N- rGO and (c) Cu/N-rGO.

Table 1. EDX analysis for GO, N-rGO and Cu/N-rGO.

Element	C (%)	O (%)	N (%)	Cu (%)
GO	45.67	54.33	0	0
N-rGO	78.17	15.85	5.98	0
Cu/N-rGO	76.06	14.86	7.22	1.86

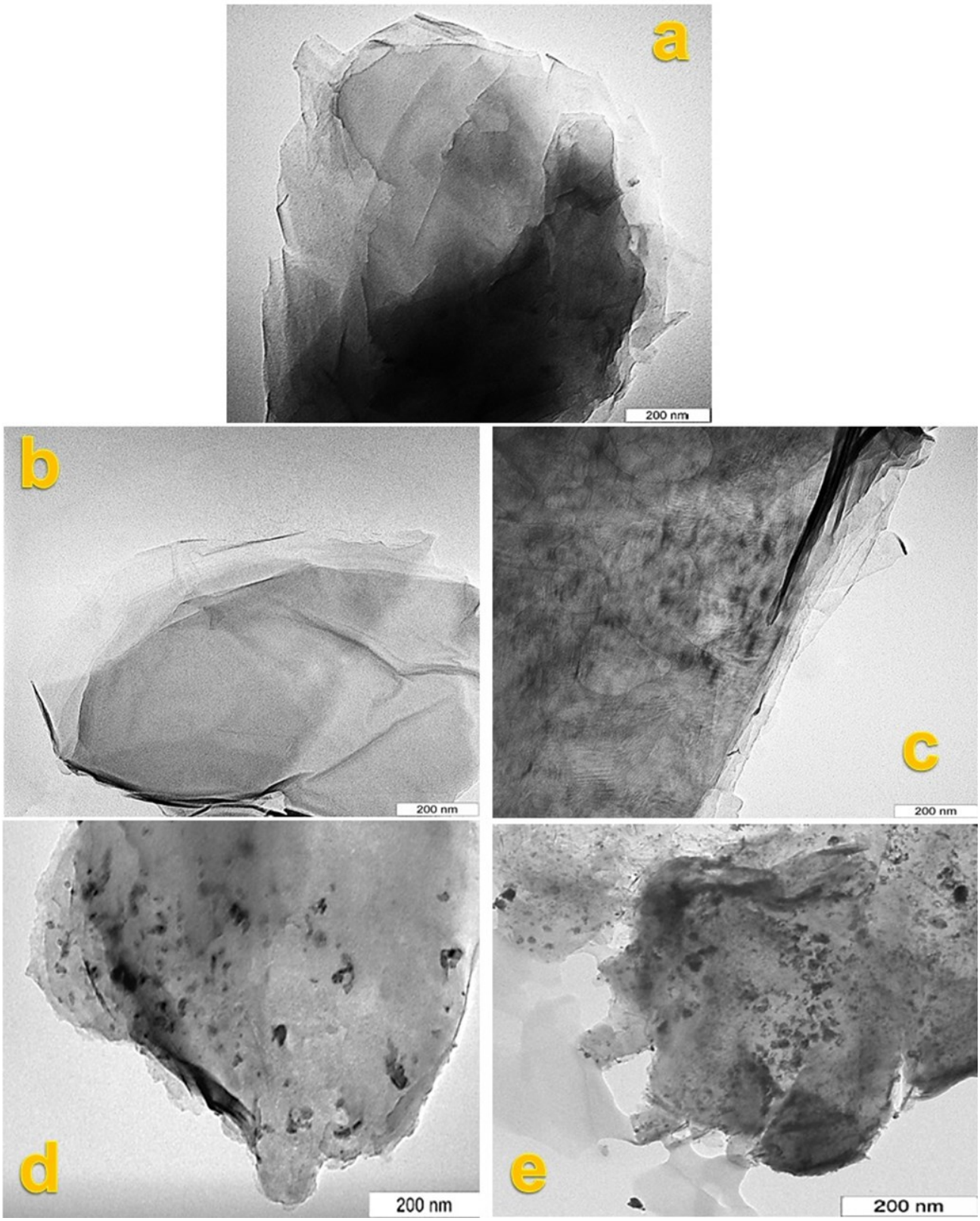

Figure 3. TEM of (a) GO, (b, c) N-rGO and (d, e) Cu/N-rGO.

served is probably due to the evaporation of the adsorbed water and the presence of such oxygen components [26].

Supporting metal nanoparticles on the graphene sheets could prevent the formation of stacked graphitic structures since the metal nanoparticles can act as spacers to increase the distance between the sheets. This could lead to increasing the surface area of the nanoparticle-graphene sheets. These materials may have promising potential applications in catalysis [27].

In Figure 5, the weight loss in the range of 150−280 °C for the Cu/N-rGO can be attributed to the combustion of the carbon skeleton of the graphene. At a temperature > 280 °C, there was no further loss of weight which is an indication that the Cu/N-rGO catalyst is in its pure form. It is obvious that the Cu/N-rGO is more thermally stable compared to GO and N-rGO [28].

3.4 XRD Analysis

The XRD pattern of the Cu/N-rGO is depicted in Figure 6. The crystallite of the element identified includes copper (Cu), nitrogen (N), graphite (C), and oxygen (O). The crystallite of the various elements was identified at a 2θ range of 10−145 °C. The crystallite at 2θ = 24.84°, and 58.68° can be attributed to the presence of reduced graphene oxide. At 2θ = 43.25°, and 61.70°, the crystallite phase repre-

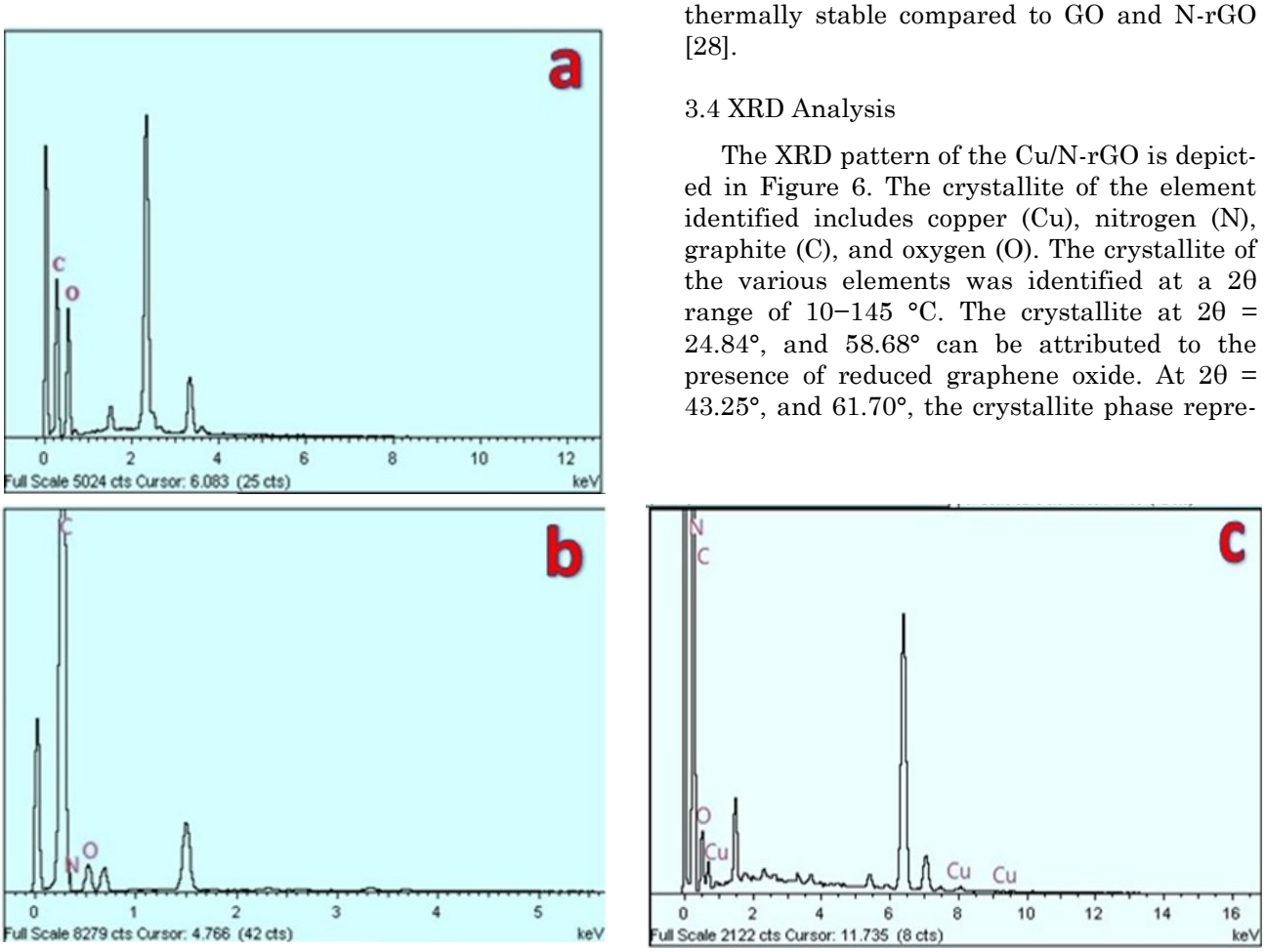

Figure 4. EDX micrograph of the (a) (GO), (b) (N-rGO) and (c) (Cu/N-rGO).

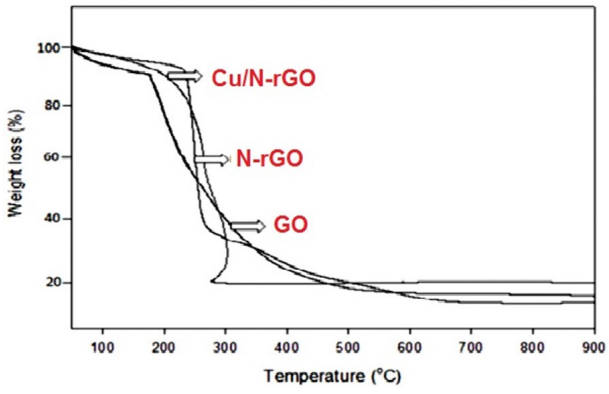

Figure 5. TGA plots for GO, N-RGO, and Cu/N-rGO.

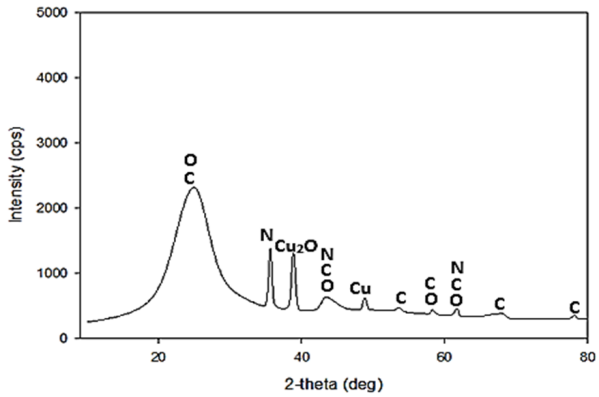

Figure 6. XRD Plots of the Cu/N-rGO catalyst.

senting the presence of the N-doped graphene oxide can be identified. The identification of copper(II) oxide is evidence at 2θ = 38.77° while copper crystallite can be identified at 2θ = 53.68°. The identification of graphite can be attributed to the peaks 2θ = 58.11°, 68.11°, and 76.1°. It can be seen that the formation of the Cu/N-rGO catalyst is evident from the XRD pattern which is consistent with that observed using the EDX analysis shown in Figure 4.

3.5 Raman Spectroscopy

The Raman spectra analysis of GO, N-rGO, and Cu/N-rGO, showing the characteristic of the D and G bands are depicted in Figure 7. The D band displayed in the catalysts can be attributed to the defects-induced zone edge phonons while the G band signifies the doubly degenerate zone center E2g mode [29]. To quantify the defects in the graphene materials, the ratio of the intensity of the D band to G band was estimated for GO, N-rGO, and Cu/N-rGO as shown in Table 2. The ID/IG ratios of 0.94, 1.02, and 1.04 obtained for the GO, N-rGO, and Cu/N-rGO, respectively, are consistent with that reported in the literature [30]. The ratios are also indications of the presence of some defects and oxygen functional groups in the as-prepared samples. The variation of the ID/IG ratio between GO and N-rGO signifies the increase in the size of C sp2 atom clusters as a result of the simultaneous reduction of GO. Interestingly, the N-doping resulted in the shifting of the G band of the rGO [31]. The estimated G peak positions of the as-prepared GO and N-rGO are approximately 1576.05 and 1573.00 cm^{-1}, respectively. Similarly, the variation in the ID/IG ratios of N-rGO and Cu/N-rGO from 1.02 to 1.04, respectively, is an indication of the removal of oxygen functionalities. Moreover, the partially ordered crystal structure of graphene as well as the presence of Cu nanoparticles on the surface of N-rGO contributes to the 3D structure of N-rGO [25].

3.6 Catalytic Activity

The catalytic activity of the Cu/N-rGO catalyst in the dehydrogenation of cyclohexanol to cyclohexanone is depicted in Figures 8 and 9. Significantly, there was an increase in the con-

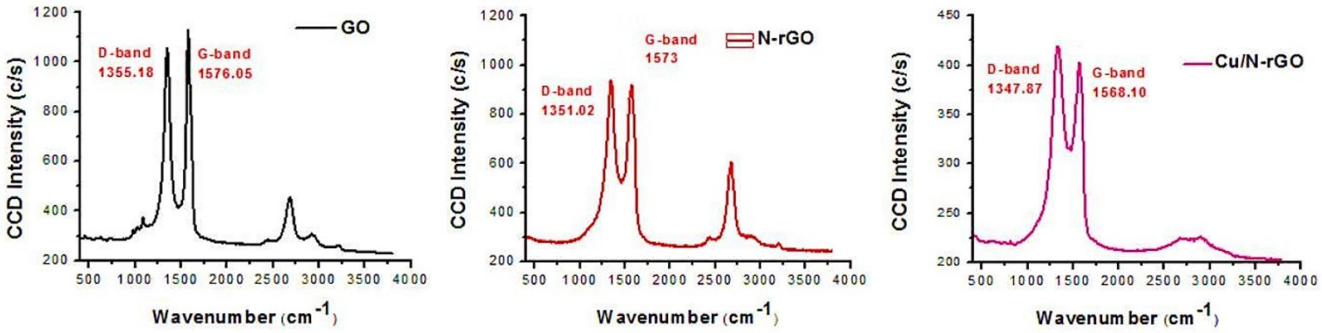

Figure 7. Raman Curves of GO, N-rGO, and Cu/N-rGO.

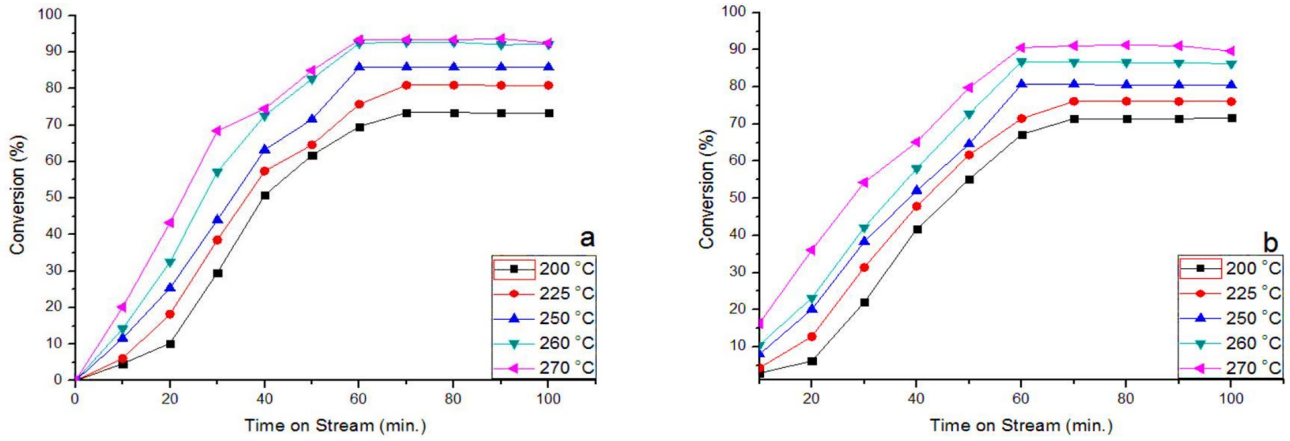

Figure 8. Conversion of cyclohexanol vs. time on stream at different operating temperatures for cyclohexanol flow rates: (a) 0.1 $mL.min^{-1}$ and (b) 0.2 $mL.min^{-1}$.

version of cyclohexanol with a rise in temperature which is consistent with Arrhenius's concept for temperature-dependent reactions, such as dehydrogenation [32]. Based on Arrhenius's concept, the activity of a temperature-dependent reaction increases with an increase in temperature. The cyclohexanol conversion increases from 73.42% at 200 °C to a maximum value of 93.6% at 270 °C, consistent with the findings of [33].

The catalytic activity of the Cu/N-rGO catalyst in terms of product yields also increases with temperature climaxing with the highest cyclohexanone yield of 78.3% at 270 °C and 0.1 mL/min. However, the selectivity of cyclohexanone using the Cu/N-rGO catalyst represented in Figure 9 decreased with a rise in temperatures and flow rates (Table 3). This could be attributed to the formation of by-products, such as cyclohexene and phenol, resulting from the influence of side reactions and subsequent dehydrogenation of cyclohexanone at elevated temperatures [34]. The improved catalytic activity can be attributed to the excellent physicochemical properties of the catalysts, such as the optimized dispersion and size distribution of Cu NPs on N-rGO. Moreover, there is a synergistic effect of the Nitrogen dopant due to the exceptional electronic properties which originate from the conjugated lone pair electron of the nitrogen and the reduced graphene oxide [35]. Synergistic effect of nitrogen-doped catalysts has been explored in various catalytic processes, such as: hydrogen evolution reaction [36] and oxygen reduction [37].

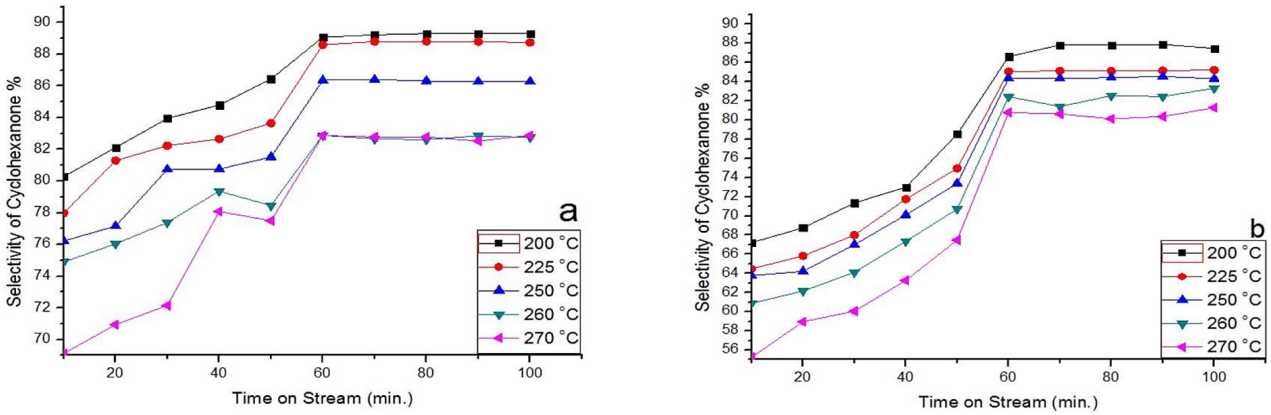

Figure 9. The selectivity of cyclohexanone vs. time on stream at different operating temperatures for cyclohexanol flow rates: (a) 0.1 mL.min^{-1} and (b) 0.2 mL.min^{-1}.

Table 2. Position and intensity of D and G bands and ID/IG ratios.

	D position (cm^{-1})	D intensity	G position (cm^{-1})	G intensity	I_D/I_G
GO	1355.18	1060	1576.05	1125.86	0.94
N-rGO	1351.02	944.	1573.00	926	1.02
Cu/N-rGO	1347.87	419.18	1568.10	402.14	1.04

Table 3. Effect of temperature on the activity and selectivity of the Cu/N-rGO catalyst for cyclohexanol flow rate of 0.1 mL.min^{-1}.

Temperature (°C)	Conversion of Cyclohexanol (%)	Selectivity of Cyclohexanone (%)	Yield of Cyclohexanone (%)
200	73.42	89.31	65.51
225	80.95	88.81	71.88
250	85.80	86.32	74.14
260	92.75	82.62	76.67
270	93.39	82.78	77.01

4. Conclusions

This study has investigated the dehydrogenation of cyclohexanol to cyclohexanone over Cu/N-rGO catalyst. In this study, the facile synthesis N-rGO by chemical reduction was demonstrated for the first time. The as-synthesized N-rGO was subsequently utilized as a support for the preparation of the Cu nanoparticles catalyst. The as-prepared Cu/N-rGO catalyst was characterized and subsequently tested in the dehydrogenation of cyclohexanol to cyclohexanone at a temperature range of 200–270 °C. The FESEM and TEM analysis showed a well-dispersed Cu NPs with small particle sizes on N-rGO sheets. The catalytic activity of the Cu NPs supported on N-rGO in dehydrogenation reactions showed that the activity in terms of conversions and yields increases with temperature. The highest cyclohexanol conversion as well as the highest cyclohexanone selectivity of 93.3% and 82.7% respectively were obtained from using the Cu/N-rGO catalyst. The improved activity and stability have been attributed to the optimized dispersion and size distribution of Cu NPs on N-rGO making a promising catalyst for the production of cyclohexanone via dehydrogenation of cyclohexanol.

Acknowledgements

The authors would like to acknowledge the Fundamental Research Grant scheme with the number 03-02-1522FR for making this research possible.

References

[1] Wang, Z., Liu, X., Rooney, D.W., Hu, P. (2015). Elucidating the mechanism and active site of the cyclohexanol dehydrogenation on copper-based catalysts: A density functional theory study. *Surface Science*, 640, 1–9.

[2] Fridman, V.Z., Davydov, A.A. (2000). Dehydrogenation of Cyclohexanol on Copper-Containing Catalysts I. The Influence of the Oxidation State of Copper on the Activity of Copper Sites. *Journal of Catalysis*, 195, 20–30.

[3] Jeon, G.S., Chung, J.S. (1994). Preparation and characterization of silica-supported copper catalysts for the dehydrogenation of cyclohexanol to cyclohexanone. *Applied Catalysis A. General,* 115(1), 29–44.

[4] Simón, E., Rosas, J.M., Santos, A., Romero, A. (2012). Study of the deactivation of copper-based catalysts for dehydrogenation of cyclohexanol to cyclohexanone, *Catalysis Today*, 187(1), 150–158.

[5] Song, Z., Ren, D., Wang, T., Jin, F., Jiang, Q., Huo, Z. (2015). Highly selective hydrothermal production of cyclohexanol from biomass-derived cyclohexanone over Cu powder. *Catalysis Today*, 274, 94–98.

[6] Ranga Rao, G., Meher, S.K., Mishra, B.G., Charan, P.H.K. (2012). Nature and catalytic activity of bimetallic CuNi particles on CeO_2 support. *Catalysis Today,* 198(1), 140–147.

[7] Chary, K.V.R., Seela, K.K., Naresh, D., Ramakanth, P. (2008). Characterization and reductive amination of cyclohexanol and cyclohexanone over Cu/ZrO_2 catalysts. *Catalysis Communications*, 9(1), 75–81.

[8] Huízar-Félix, A.M., Cruz-Silva, R., Barandiarán, J.M., García-Gutiérrez, D.I., Orue, I., Merida, D., Sepúlveda-Guzmán, S. (2016). Magnetic properties of thermally reduced graphene oxide decorated with PtNi nanoparticles. *Journal of Alloys and Compounds*, 678, 541–548.

[9] Yang, J., Shen, X., Ji, Z., Zhou, H., Zhu, G., Chen, K. (2015). In-situ growth of Cu nanoparticles on reduced graphene oxide nanosheets and their excellent catalytic performance. *Ceramics International*, 41(3), 4056–4063.

[10] Ma, J., Wang, L., Mu, X., Li, L. (2015). Nitrogen-doped graphene supported Pt nanoparticles with enhanced performance for methanol oxidation. *International Journal of Hydrogen Energy*, 40(6), 2641–2647.

[11] Fakhri, P., Jaleh, B., Nasrollahzadeh, M. (2014). Synthesis and characterization of copper nanoparticles supported on reduced graphene oxide as a highly active and recyclable catalyst for the synthesis of formamides and primary amines. *Journal of Molecular Catalysis A: Chemical*, 383-384, 17–22.

[12] Lee, D.W., Seo, J.W. (2011). Preparation of carbon nanotubes from graphite powder at room temperature. *arXiv preprint arXiv*. 1007, 1−10.

[13] Ning, R., Tian, J., Asiri, A.M., Qusti, A.H., Al-Youbi, A.O., Sun, X. (2013). Spinel $CuCo_2O_4$ nanoparticles supported on n-doped reduced graphene oxide: A highly active and stable hybrid electrocatalyst for the oxygen reduction reaction. *Langmuir*, 29(43), 13146–13151.

[14] Loryuenyong, V., Totepvimarn, K., Eimburanapravat, P., Boonchompoo, W., Buasri, A. (2013). Preparation and Characterization of Reduced Graphene Oxide Sheets via Water-Based Exfoliation and Reduction Methods. *Advances in Materials Science and Engineering*, 2013, 1-6.

[15] Seung Hun, H., Hae-Mi, J., Sung-Ho, C. (2010). X-ray Diffraction Patterns of Thermally-reduced Graphenes. *Journal of the Korean Physical Society*, 57(61), 1649−1652.

[16] Ismail, N., Madian, M., El-Shall, M.S. (2015). Reduced graphene oxide doped with Ni/Pd nanoparticles for hydrogen storage application. *Journal of Industrial and Engineering Chemistry*, 30, 328–335.

[17] Fu, C., Zhao, G., Zhang, H., Li, S. (2013). Evaluation and Characterization of Reduced Graphene Oxide Nanosheets as Anode Materials for Lithium-Ion Batteries. *International Journal of Electrochemical Sciences*, 8, 6269–6280.

[18] Stankovich, S., Dikin, D.A., Piner, R.D., Kohlhaas, K.A., Kleinhammes, A., Jia, Y., Wu, Y., Nguyen, S.T., Ruoff, R.S. (2007). Synthesis of graphene-based nanosheets via chemical reduction of exfoliated graphite oxide. *Carbon*, 45(7), 1558–1565.

[19] Alanyalioglu, M., Segura, J.J., Oro-Sol, J., Casan-Pastor, N. (2012). The synthesis of graphene sheets with controlled thickness and order using surfactant-assisted electrochemical processes. *Carbon*, 50(1), 142–152.

[20] Zhang, W., Wu, P., Li, Z., Yang, J. (2011). First-principles thermodynamics of graphene growth on Cu surfaces. *Journal of Physical Chemistry C*, 115, 17782–17787.

[21] Zhen-Jiang, L., Mao-wen, X., Shu-Juan, B., Kehfarn, T., Hui, C., Chang-Jun, C., Chen-Chen, J., Qiang, Z. (2013). Facile preparation of nitrogen-doped graphene as a metal-free catalyst for oxygen reduction reaction. *J Mater Sci.*, 48(10), 8101–8107.

[22] Yang, J., Shen, X., Ji, Z., Zhou, H., Zhu, G., Chen, K. (2015). In-situ growth of Cu nanoparticles on reduced graphene oxide nanosheets and their excellent catalytic performance. *Ceramics International*, 41(3), 4056–4063.

[23] Neha, B. (2012). Synthesis and Characterization of Exfoliated Graphite/ABS Composites. *Open Journal of Organic Polymer Materials*, 02(04), 75–79.

[24] Li, Y., Ye, K. Cheng, K., Cao, D., Pan, Y., Kong, S., Wang, G. (2014). Anchoring CuO nanoparticles on nitrogen-doped reduced graphene oxide nanosheets as electrode material for supercapacitors. *Journal of Electroanalytical Chemistry*, 727, 154–162.

[25] Jia, Z., Chen, T., Wang, J., Ni, J., Li, H., Shao, X. (2015). Synthesis, characterization and tribological properties of Cu/reduced graphene oxide composites. *Tribology International*, 88, 17–24.

[26] Shateesh, B., Markad, G.B., Haram, S.K. (2016) Nitrogen doped Graphene Oxides as an efficient electrocatalyst for the Hydrogen evolution Reaction; Composition based Electrodics Investigation. *Electrochemical Acta*, 200, 53–58.

[27] Hassan, H.M.A., Abdelsayed, V., Khder, A.E.R.S., AbouZeid, K.M., Terner, J., El-Shall, M.S., Al-Resayes, S.I., El-Azhary A.A. (2009). Microwave synthesis of graphene sheets supporting metal nanocrystals in aqueous and organic media. *Journal of Materials Chemistry,* 19(23), 3832−3837.

[28] Ding, T., Tian, H., Liu, J., Wu, W., Zhao, B. (2016). Effect of promoters on hydrogenation of diethyl malonate to 1,3-propanediol over nano copper-based catalysts. *CATCOM,* 74, 10–15.

[29] Shahriary, L., Athawale, A.A. (2014). Graphene Oxide Synthesized by using Modified Hummers Approach. *International Journal of Renewable Energy and Environmental Engineering*, 02(01), 58–63.

[30] Shao, G., Lu, Y., Wu, F., Yang, C., Zeng, F., Wu, Q. (2012). Graphene oxide: The mechanisms of oxidation and exfoliation. *Journal of Materials Science*, 47(10), 4400–4409.

[31] He, D., Jiang, Y., Lv, H., Pan, M., Mu, S. (2013). Nitrogen-doped reduced graphene oxide supports for noble metal catalysts with greatly enhanced activity and stability. *Applied Catalysis B: Environmental,* 132-133, 379–388.

[32] Ayodele, B.V., Hossain, M.A., Chong, S.L., Soh, J.C., Abdullah, S., Khan, M.R., Cheng, C.K. (2016). Non-isothermal kinetics and mechanistic study of thermal decomposition of light rare earth metal nitrate hydrates using thermogravimetric analysis. *Journal of Thermal Analysis and Calorimetry*, 125(1), 423−435.

[33] Popova, M., Dimitrov, M., Santo, V.D., Ravasio, N., Scotti, N. (2012). Dehydrogenation of cyclohexanol on copper containing catalysts: The role of the support and the preparation method. *Catalysis Communications*, 17, 150–153.

[34] Simon, E., Pardo, F., Lorenzo, D., Santos, A., Romero, A. (2012). Kinetic model of 2-cyclohexenone formation from cyclohexanol and 2-cyclohexenol dehydrogenation. *Chemical Engineering Journal,* 192, 129–137.

[35] Li, M., Zhang, L., Xu, Q., Niu, J., Xia, Z. (2014). N-doped graphene as catalysts for oxygen reduction and oxygen evolution reactions: Theoretical considerations. *Journal of catalysis*, 314, 66−72.

[36] Li, D.J., Maiti, U.N., Lim, J., Choi, D.S., Lee, W.J., Oh, Y., Song, H., Zhong, Y., Kim, S.O. (2014). Molybdenum sulfide/N-doped CNT forest hybrid catalysts for high-performance hydrogen evolution reaction. *Nano letters*, 14(3), 1228−1233.

[37] Peng, H., Mo, Z., Liao, S., Liang, H., Yang, L., Luo, F., Song, H., Zhong, Y., Zhang, B. (2013). High performance Fe-and N-doped carbon catalyst with graphene structure for oxygen reduction. *Scientific Reports,* 3, 1-7.